MINIREVIEWS

Nanomaterials

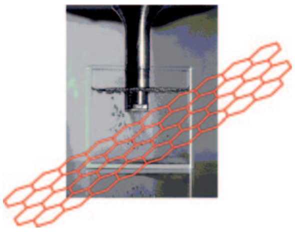

Sound—action! Inexpensive graphitic precursors can be transformed into invaluable graphenes (both single and few layers) using ultrasonication as the key step. This safe wet chemistry enables rapid dispersion and formation of stable colloids (see figure). This minireview unveils the rich and sound science behind the lab trick.

Asymmetric Organocatalysis

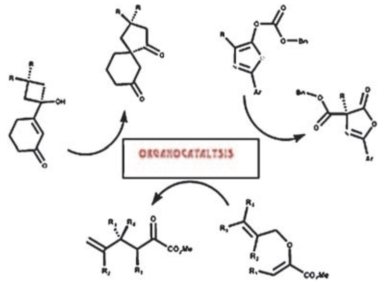

Organic catalysts can (re)arrange it! Rearrangement reactions often allow the construction of otherwise hard-to-access molecular frameworks, but are not very amenable to asymmetric catalysis (see scheme). Recent research has shown that organocatalytic modes of activation can be successfully applied to a variety of rearrangements. The advances achieved so far in asymmetric organocatalytic rearrangement reactions are summarized herein.

Homogeneous Catalysis

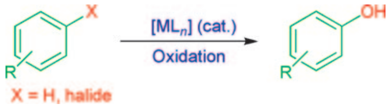

The many routes to phenols! This minireview highlights recent strategies to synthesize hydroxylated arenes by transition-metal-catalyzed oxidation of arenes by C−H activation or cross-coupling methodologies (see scheme).

COMMUNICATIONS

Asymmetric Catalysis

Improving the structural scope: A catalytic asymmetric 1,3-dipolar cycloaddition involving α-iminonitriles as azomethine precursors has been developed. In the presence of AgOAc/Taniaphos as the catalyst system the reaction of α-iminonitriles with dimethyl fumarate and *N*-methyl maleimide affords 2-cyanopyrrolidines with good *endo* selectivity and enantioselectivity (68–≥99 % *ee*; see scheme).

Metal–Organic Frameworks

X.-J. Kong, H. Zhang, H.-X. Zhao, Y.-P. Ren, L.-S. Long,* Z. Zheng,* G. S. Nichol, R.-B. Huang, L.-S. Zheng* .... 5292 – 5296

Framework Solids Possessing Both Hydrophobic and Hydrophilic Pores Constructed by Face-Sharing Keplerate-Type Heterometal–Organic Polyhedra

Interesting MOPs! Two isostructural framework structures built from novel Keplerate-type 3d–4f heterometal–organic polyhedra (HMOPs), both with hydrophilic and hydrophobic pores of nanoscopic dimensions, have been obtained. The 36-metal HMOPs display an aesthetically pleasing double-Archimedean solid structure characterized by a cuboctahedron encapsulating a rhombicuboctahedron (see figure).

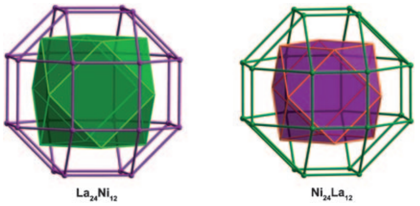

Fluorescent Probes

T.-I. Kim, M. S. Jeong, S. J. Chung, Y. Kim** .... 5297 – 5300

An Iminocoumarin-Based Fluorescent Probe for the Selective Detection of Dual-Specific Protein Tyrosine Phosphatases

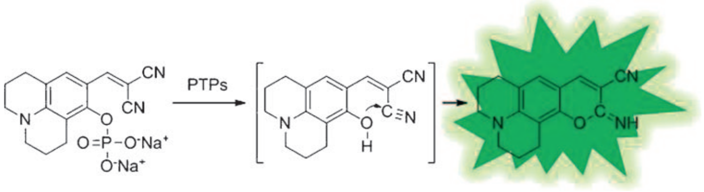

Seeing is believing: A fluorescent probe for monitoring the activity of dual-specific protein tyrosine phosphatases (PTPs) has been developed (see scheme). Selective enzymatic hydrolysis and subsequent intramolecular cyclization results in a highly fluorescent iminocoumarin fluorophore.

Acrylonitriles

M. Ma, G. Hou, T. Sun, X. Zhang, W. Li, J. Wang, X. Zhang** .... 5301 – 5304

Highly Efficient Rh$^{\mathrm{I}}$-Catalyzed Asymmetric Hydrogenation of β-Amino Acrylonitriles

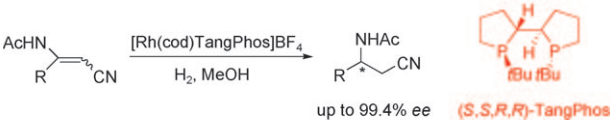

It takes two to TangPhos: β-Amino acrylonitriles can be readily prepared from acetonitriles. Both of the *E/Z* isomers undergo hydrogenation with excellent enantioselectivity by using the Rh–TangPhos (TangPhos = 1,1′-di-*tert*-butyl-(2,2′)-diphospholane) catalyst system. The products, chiral β-amino nitriles, are valuable chiral building blocks for many drugs.

Self-Assembly

E. K. Chung, E. Lee, Y.-b. Lim, M. Lee** .... 5305 – 5309

Cyclic Peptide Facial Amphiphile Preprogrammed to Self-Assemble into Bioactive Peptide Capsules

Programmed assembly: A unique supramolecular building block, a cyclic peptide facial amphiphile, predestined to self-assemble into a nanocapsule structure, has been developed (see figure). This general strategy will allow the easy construction of a variety of bioactive nanocapsules.

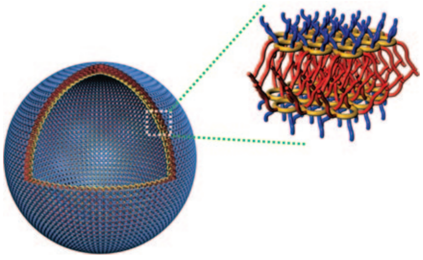

Cycloisomerization

S. Y. Kim, Y. K. Kang, Y. K. Chung** .... 5310 – 5313

Rh$^{\mathrm{I}}$-Catalyzed Cycloisomerization of Vinyl Bicyclopropyl Compounds to Azabicyclo[3.2.2]nona-2,8-dienes

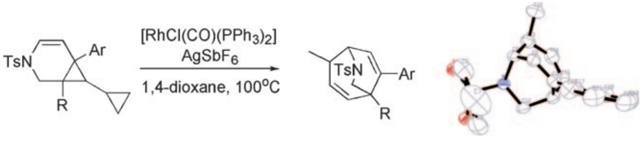

Important class: Nitrogen-containing heterobicycles are an important structural motif ubiquitous in natural alkaloids. We found that azabicyclo-[3.2.2]nona-2,8-dienes can be synthesized from vinyl bicyclopropropyl derivatives in the presence of a Rh$^{\mathrm{I}}$ catalyst (see scheme). Syntheses of such compounds and an investigation into the reaction mechanism through DFT calculations are presented.

Frontiers of Chemistry:
From Molecules to Systems

A One-Day Symposium

On 21st May 2010 in Paris

at the Maison de la Chimie
(near the Eiffel Tower and Les Invalides)

Celebrating 10 Years of

Speakers


Gerhard Ertl
Nobel Prize 2007


Jean-Marie Lehn
Nobel Prize 1987


Roger Y. Tsien
Nobel Prize 2008


Ada Yonath
Nobel Prize 2009


Luisa De Cola


Alan R. Fersht


Marc Fontecave


Michael Grätzel


Michel Orrit


Nicolas Winssinger

Scientific committee

E. Amouyal, M. Che,
F. C. De Schryver,
A. R. Fersht, P. Gölitz,
J. T. Hynes, J.-M. Lehn

Posters

will be displayed also online from 1st April

www.chembiophyschem.org

Topics

catalysis, biochemical imaging, chemical biology, bionanotechnology, proteomics, spectroscopy, solar cells

Organized by

ChemPubSoc Europe

Société Chimique de France

Partner of the event sanofi aventis
Because health matters

WILEY-VCH

557101001

FULL PAPERS

Prebiotic Chemistry

Proteins in an RNA world: Gly, Ala, Ile, Lys and His form under the same set of putative prebiotic conditions, and a peptide composed of just these amino acids tetramerises to adopt a well-folded four-helix bundle (see figure). In the presence of certain divalent cations, this molecule efficiently and specifically degrades RNA. These results suggest that peptides and divalent cations with RNase activity could have co-inhabited the RNA world.

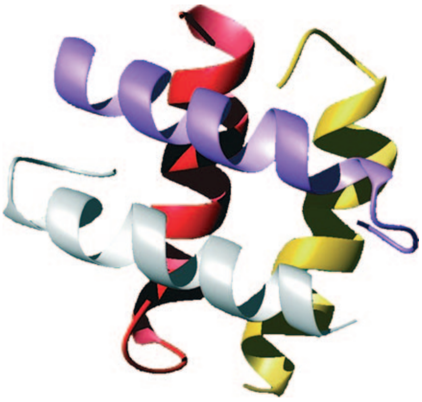

Metal–Ligand Interactions

Weakness and strength: Whereas Au^I interacts weakly with the covering arene ring in complexes with dialkylbiphenylphosphane ligands, strong interactions have been found in Ag^I and Cu^I complexes. Dialkylbiphenylphosphane arene–Ag^I complexes, such as the example illustrated (Cy = cyclohexyl), have the strongest Ag^I–arene bonds known.

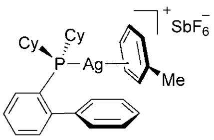

Asymmetric Catalysis

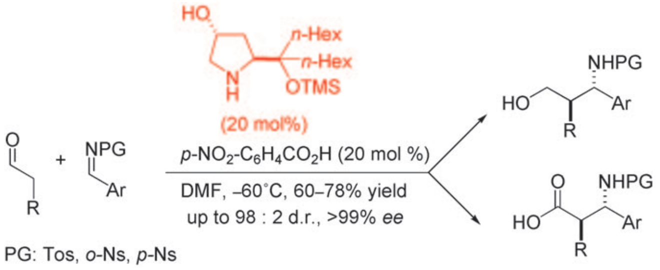

A three-component arrangement is best! Highly enantioselective *anti*-Mannich reaction of aldehydes with *N*-sulfonyl imines (see scheme) may be achieved by using a 4-hydroxypyrrolidine-based bifunctional catalyst in combination with an external Brønsted acid. Significantly, the present catalyst system is very efficient with aromatic aldehyde-derived imines, a type of Mannich acceptor that has rarely been employed in previous enamine-based *anti*-Mannich reactions.

Photoinduced Electron Transfer

*Y. Takano, M. Á. Herranz, N. Martín,**
*G. de Miguel Rojas, D. M. Guldi,**
*I. E. Kareev, S. H. Strauss,**
O. V. Boltalina, T. Tsuchiya,*
*T. Akasaka** .... 5343 – 5353

Electron Donor–Acceptor Interactions in Regioselectively Synthesized exTTF$_2$–C$_{70}$(CF$_3$)$_{10}$ Dyads

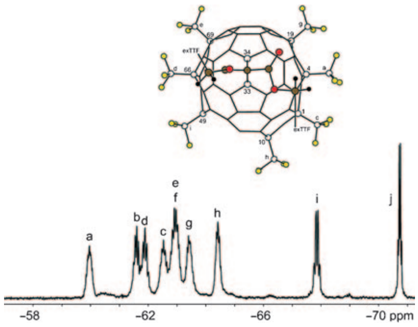

Fluoro-fying fullerenes: In the first example of trifluoromethylated fullerene-based donor–acceptor dyads, exTTF$_2$–C$_{70}$(CF$_3$)$_{10}$ was prepared in high yield by the regioselective reaction of an exTTF-based malonate under standard Bingel–Hirsch conditions (see figure). Various photophysical techniques were employed to assess the intramolecular electronic interactions taking place after photoexcitation, which resulted in a charge-separated state with a lifetime between 23 and 289 ps.

Organocatalysis

A.-N. R. Alba, X. Companyó,
*G. Valero, A. Moyano,**
*R. Rios** .... 5354 – 5361

Enantioselective Organocatalytic Addition of Oxazolones to 1,1-Bis(phenylsulfonyl)ethylene: A Convenient Asymmetric Synthesis of Quaternary α-Amino Acids

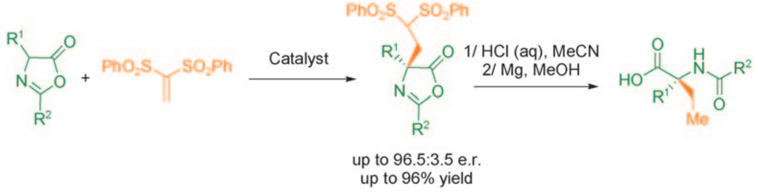

Quaternary amino acids made easy! Oxazolones react with 1,1-bis(phenylsulfonyl)ethylene under catalysis by simple chiral bases or thioureas to afford α,α-disubstituted α-amino acid derivatives with excellent yields and enantioselectivities (see scheme).

Programmed Self-Assembly

M. Endo, T. Sugita, Y. Katsuda,*
*K. Hidaka, H. Sugiyama** .. 5362 – 5368

Programmed-Assembly System Using DNA Jigsaw Pieces

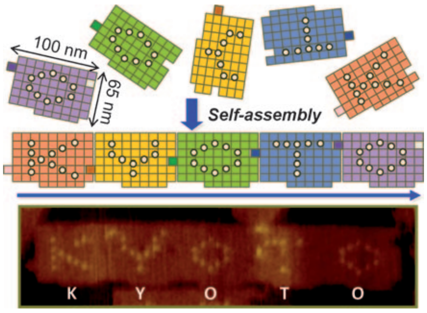

Pieces of the puzzle! A novel method for the programmed assembly of multiple DNA origami structures was developed by using designed DNA rectangles that have sequence-programmed connectors. DNA jigsaw pieces self-assembled to form predesigned 1D assemblies according to the connective hybridization strands, shape, and π-stacking interactions. In addition, DNA jigsaw pieces with alphabet letters were arranged to display three-, four-, and five-letter words (see graphic).

Molecular Motion

A.-M. Stadler, J. Ramírez,
*J.-M. Lehn** .... 5369 – 5378

Control of Relative Direction and Amplitude in Extension/Contraction Motions of Molecular Strands Induced by Ion Binding

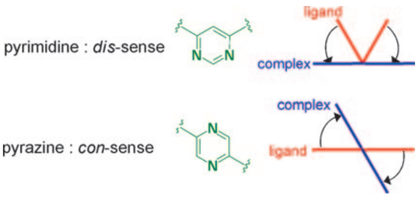

On the move: The amplitude of the motion induced by metal-ion binding and release from aza-heterocycles connected by hydrazone groups and the relative directions of the motions are controlled by the nature of the heterocyclic units. Motions around a central 4,6-disubstituted pyrimidine are *dis*-sense motions, whereas *con*-sense motions occur around a central 2,5-disubstituted pyrazine unit (see picture).

In and out: A study of NH_3 synthesis as a probe reaction suggests the Ru atom located on the exterior carbon nanotube (CNT) surface is likely to have a higher electron density, which could be the reason for the higher catalytic activity, than the inside Ru (see figure). This indicates that the electron transfer from the concave inner to the convex outer surface could play a role in catalysis.

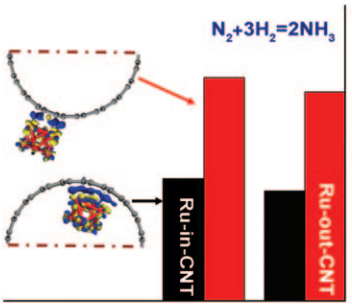

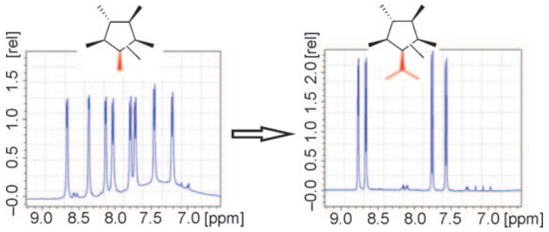

Shift it: The impact of amino acid side chain mutations on the backbone of cyclic peptides, especially *N*-methylated cyclic peptides, has been investigated. It could be shown that the unwanted appearance of *cis* amide bonds can be suppressed by the introduction of β-branched amino acid side chains (see figure), which strongly shift the equilibrium between *cis* and *trans* towards the all-*trans* conformation.

Comparing calculations: The π···π-stacking and C–H···π interactions of model transition-metal aromatic compounds (see figure) are examined by using ab initio and DFT methods.

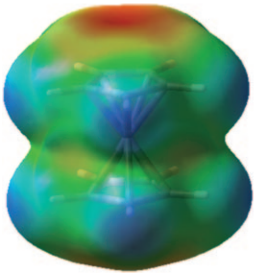

Dynamic discoveries! In this paper, we describe, at the molecular level, the thermal unfolding of a helical peptide, QK_{L10A}, by using experimental and computational techniques. The comparison of the structures at 298 and 313 K shows that QK_{L10A} at 313 K retains a single central helix turn, representing the most probable site for the helix nucleation, which then propagates toward the two terminal ends (see graphic).

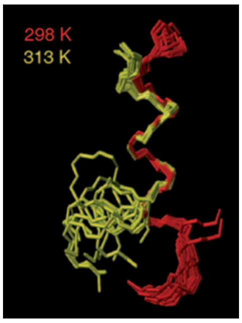

Gas-Phase Thermochemistry

*E. P. A. Couzijn, E. Zocher, A. Bach, P. Chen** 5408–5415

Gas-Phase Energetics of Reductive Elimination from a Palladium(II) N-Heterocyclic Carbene Complex

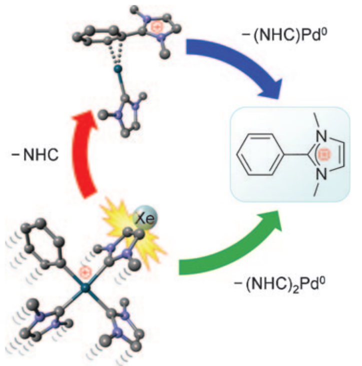

Reductive elimination of 2-phenylimidazolium competes with dissociation of an N-heterocyclic carbene (NHC) from the complex $[(NHC)_3PdPh]^+$, as was studied by tandem mass spectrometry. The resulting three-coordinate complex can again generate the same imidazolium species (see scheme). Activation energies were measured for all three processes and compared with the results of density functional calculations.

Click Chemistry

*H. S. Mader, M. Link, D. E. Achatz, K. Uhlmann, X. Li, O. S. Wolfbeis** 5416–5424

Surface-Modified Upconverting Microparticles and Nanoparticles for Use in Click Chemistries

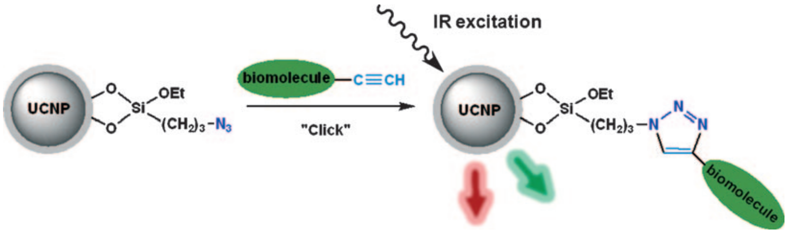

Clickable upconverting nanoparticles (UCNPs): $NaYF_4$:Yb,Er nanoparticles were coated with silica and functionalized with azido and alkyne groups, respectively. This enables selective coupling to biotin, maleimides, or fluorescent dyes by means of a click reaction (see scheme). If laser-excited with near-infrared light at 980 nm, the nanoparticles display bright visible luminescence.

Reductive C–C Coupling

J. A. Cabeza, I. del Río, E. Pérez-Carreño, V. Pruneda* 5425–5436

Reductive Dimerization of Triruthenium Clusters Containing Cationic Aromatic N-Heterocyclic Ligands

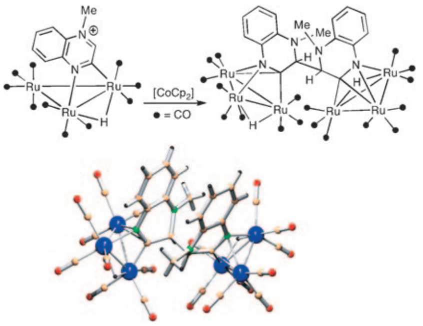

Intermolecular C–C bond formation: Cobaltocene reduces the title clusters to odd-electron trinuclear intermediates that end in hexanuclear derivatives containing novel dimeric nonaromatic N-heterocyclic ligands. The cationic character of the aromatic ligands of the starting complexes, which have ligand-based LUMOs, is responsible for the observed reactivity.

Heterogeneous Catalysis

M. L. H. Mantel, A. T. Lindhardt, D. Lupp, T. Skrydstrup** 5437–5442

Pd-Catalyzed C–N Bond Formation with Heteroaromatic Tosylates

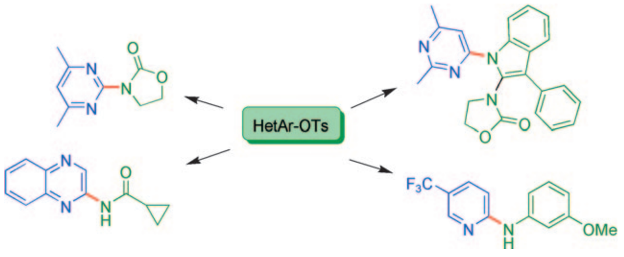

The more nitrogens the merrier: Palladium(0)-catalyzed amidations were performed with a variety of heteroaromatic tosylates (HetAr-OTs; see scheme) in combination with amides, including oxazolidinones, lactams, anilines, indoles and one cyclic urea. These reactions are highly efficient, providing products with high diversity and one or more heterocyclic moieties.

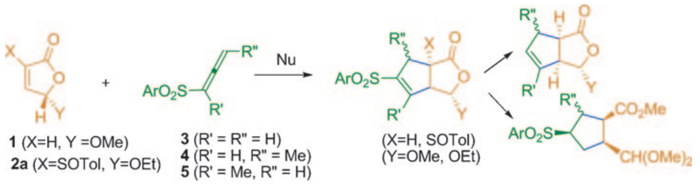

Abnormal allenes: Activation of allenylsulfones with phosphines or sulfinates and further reaction with 5-alkoxyfuran-2(5*H*)-ones or their (*S*)-3-*p*-tolylsulfinyl derivatives affords bicyclic adducts with the sulfonyl group at C-5, in a completely regio- and π-facial selective manner (see scheme; Tol = tolyl). The reaction mechanism is different to that proposed for Lu's reaction of allenoates and furanones.

Asymmetric Synthesis

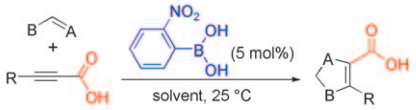

Acid phobia is over: Free, unsaturated carboxylic acids can participate directly in dipolar cycloadditions with azides, nitrile oxides, and nitrones by using mild boronic acid catalysis at room temperature to give readily isolated heterocyclic products (see scheme).

Heterocycles

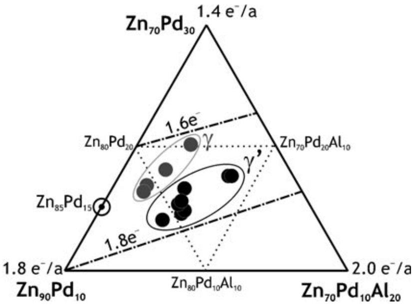

Confirmed existence: Novel ternary phases, $(Pd_{1-x}Zn_x)_{18}(Zn_{1-y}Al_y)_{86-\delta}$ ($0 \leq x \leq 0.162$, $0.056 \leq y \leq 0.088$, $0 \leq \delta \leq 4$), which adopt a superstructure of the γ-brass type (called γ′-brass), have been synthesized from the elements at 1120 K. The distribution of γ- (*cI*52) and γ′-phases (*cF*400-*cF*416) characterized in the Zn-rich portion of Pd–Zn–Al phase diagram are depicted. Electron per atom (e^-/a) values for the corners, as well as lines for 1.6 and 1.8 e^-/atom are also given.

Hume-Rothery Compounds

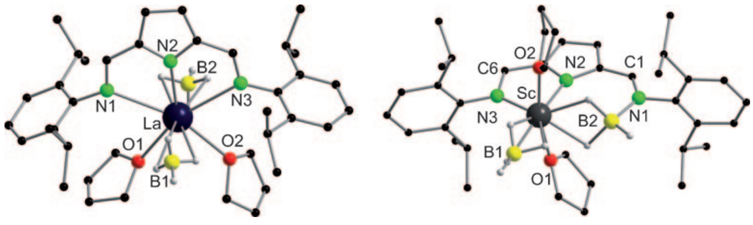

Unusual coordination and reactivity: Depending on the ionic radius of the central metal atom, the BH_4^- group, which usually reacts in lanthanide chemistry as a pseudohalide, can be involved in redox chemistry. The resulting product contains an $N-BH_3$ unit that binds in an unusual η^2 fashion onto the metal atom (see graphic). The Nd complexes were used as Ziegler–Natta catalysts for the polymerization of 1,3-butadiene to poly(*cis*-1,4-butadiene).

Rare-Earth-Metal Complexes

Spectroelectrochemistry

*J. Aragó, P. M. Viruela, E. Ortí,**
R. Malavé Osuna, B. Vercelli, G. Zotti,
V. Hernández, J. T. López Navarrete,**
J. T. Henssler, A. J. Matzger, Y. Suzuki,
S. Yamaguchi .... 5481 – 5491

💻 **Neutral and Oxidized Triisopropylsilyl End-Capped Oligothienoacenes: A Combined Electrochemical, Spectroscopic, and Theoretical Study**

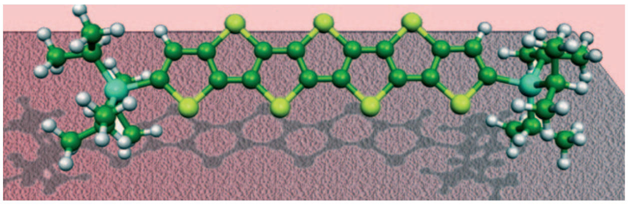

Rigid molecular structures: Triisopropylsilyl end-capped oligothienoacenes form stable cation species and present absorption and fluorescence spectra with well-resolved vibronic structures, due to the rigidity of the molecular structure (see figure). The vibronic progressions observed at low temperature are due to vibronic coupling with normal modes associated with a collective stretching of the carbon backbone (1525 cm^{-1}) and to the in-plane bending of the thiophene rings (480 cm^{-1}).

Prion proteins

N.-S. Lin, J. C.-H. Chao, H.-M. Cheng,
F.-C. Chou, C.-F. Chang, Y.-R. Chen,
Y.-J. Chang, S.-J. Huang,
*J. C. C. Chan** .... 5492 – 5499

💻 **Molecular Structure of Amyloid Fibrils Formed by Residues 127 to 147 of the Human Prion Protein**

Amyloid fibrils: We present a structural model of an in-register parallel β sheet for amyloid fibrils formed from human prion protein (see figure). A simple solid-state NMR spectroscopy technique was developed to identify solvent-protected backbone amide protons in an H/D exchange experiment without disaggregating the amyloid fibrils, from which we find that proline residue P_{137} does not disrupt the β-sheet structure from G_{127} to G_{142}.

---

* Author to whom correspondence should be addressed

💻 Supporting information on the WWW (see article for access details).

VIP Full Papers labeled with this symbol have been judged by two referees as being "very important papers".

A video clip is available as Supporting Information on the WWW (see article for access details).

SERVICE